electronics

MDPI

Article

Game-Theory-Based Design and Analysis of a Peer-to-Peer Energy Exchange System between Multi-Solar-Hydrogen-Battery Storage Electric Vehicle Charging Stations

Lijia Duan [1], Yujie Yuan [2,*], Gareth Taylor [1] and Chun Sing Lai [1,*]

[1] Department of Electronic and Electrical Engineering, Brunel University London, London UB8 3PH, UK; lijia.duan@brunel.ac.uk (L.D.); gareth.taylor@brunel.ac.uk (G.T.)
[2] School of Air Traffic Management, Civil Aviation University of China, Tianjin 300300, China
* Correspondence: yjyuan@cauc.edu.cn (Y.Y.); chunsing.lai@brunel.ac.uk (C.S.L.)

Abstract: As subsidies for renewable energy are progressively reduced worldwide, electric vehicle charging stations (EVCSs) powered by renewable energy must adopt market-driven approaches to stay competitive. The unpredictable nature of renewable energy production poses major challenges for strategic planning. To tackle the uncertainties stemming from forecast inaccuracies of renewable energy, this study introduces a peer-to-peer (P2P) energy trading strategy based on game theory for solar-hydrogen-battery storage electric vehicle charging stations (SHS-EVCSs). Firstly, the incorporation of prediction errors in renewable energy forecasts within four SHS-EVCSs enhances the resilience and efficiency of energy management. Secondly, employing game theory's optimization principles, this work presents a day-ahead P2P interactive energy trading model specifically designed for mitigating the variability issues associated with renewable energy sources. Thirdly, the model is converted into a mixed integer linear programming (MILP) problem through dual theory, allowing for resolution via CPLEX optimization techniques. Case study results demonstrate that the method not only increases SHS-EVCS revenue by up to 24.6% through P2P transactions but also helps manage operational and maintenance expenses, contributing to the growth of the renewable energy sector.

Keywords: electric vehicle charging station; photovoltaic; hydrogen storage system; battery storage; peer-to-peer energy trading; game theory

Citation: Duan, L.; Yuan, Y.; Taylor, G.; Lai, C.S. Game-Theory-Based Design and Analysis of a Peer-to-Peer Energy Exchange System between Multi-Solar-Hydrogen-Battery Storage Electric Vehicle Charging Stations. *Electronics* **2024**, *13*, 2392. https://doi.org/10.3390/electronics13122392

Academic Editors: Hanqing Yang, Jiajia Yang, Zening Li and Zhengmao Li

Received: 17 May 2024
Revised: 16 June 2024
Accepted: 17 June 2024
Published: 19 June 2024

1. Introduction

Electric vehicles (EVs) are at the forefront of the global shift towards sustainable transportation, offering a cleaner, more energy-efficient alternative to traditional engine vehicles [1–3]. EVs leverage advances in battery technology, electric motors, and power electronics to provide a driving experience that is not only environmentally friendly but increasingly competitive in terms of performance, range, and cost. As governments worldwide implement policies to reduce carbon emissions and consumers become more eco-conscious, the adoption of EVs is accelerating, supported by expanding infrastructure for charging and a growing recognition of their role in mitigating climate change [4,5]. Embracing the future of mobility, EVs represent a key component in the transition to a low-carbon economy, promising a greener, more sustainable future for transportation.

Amid the swiftly advancing energy transition, multi-energy electric vehicle charging stations (EVCSs) are emerging as crucial infrastructure components for promoting sustainable transportation. These EVCSs, which harness various renewable energy technologies, including solar, wind, hydrogen, and battery storage, provide versatile charging solutions that help stabilize grid loads and optimize energy utilization. Equipped with advanced management systems, multi-energy EVCSs can dynamically adjust charging power and methods in response to real-time variations in energy supply and demand. This capability not only boosts energy efficiency and cuts operational costs but also significantly supports

the ecological transformation of the power grid [6]. As trailblazers in the new era of mobility, EVs play a key role in the shift towards a low-carbon economy, heralding a more sustainable and greener future for transportation.

The shift toward sustainable energy systems is gaining momentum, and in this evolving situation, EVCSs equipped with diverse energy options—such as solar energy, hydrogen storage systems, and battery storage—are becoming increasingly critical. The integration of these varied energy sources necessitates the development of innovative management strategies to ensure efficient operation, economic viability, and reliability of the power supply. Within this framework, game theory and mixed-integer linear programming (MILP) are being effectively utilized to design and analyze peer-to-peer (P2P) energy exchange systems. These analytical approaches help optimize the distribution and utilization of resources, ensuring that EVCSs can meet demand flexibly and sustainably.

Figure 1 shows a solar-hydrogen-storage-integrated electric vehicle charging station (SHS-EVCS), which utilizes the combined capabilities of photovoltaic panels, a hydrogen storage system, and battery storage to charge electric vehicles. This station features a solar array that captures sunlight and transforms it into electrical energy. This energy can either be used directly to charge EVs or be fed into the grid and stored in battery reserves for later use. For hydrogen energy storage, the system incorporates an electrolyzer that splits water molecules into hydrogen and oxygen. The hydrogen is then compressed and stored, ready to be used when needed. During peak demand periods, this hydrogen is converted back into electricity through a fuel cell to power EVs. Additionally, a battery storage unit captures any excess energy from the solar array or the fuel cell, ensuring a consistent energy supply to charge EVs even when the primary renewable sources are inactive.

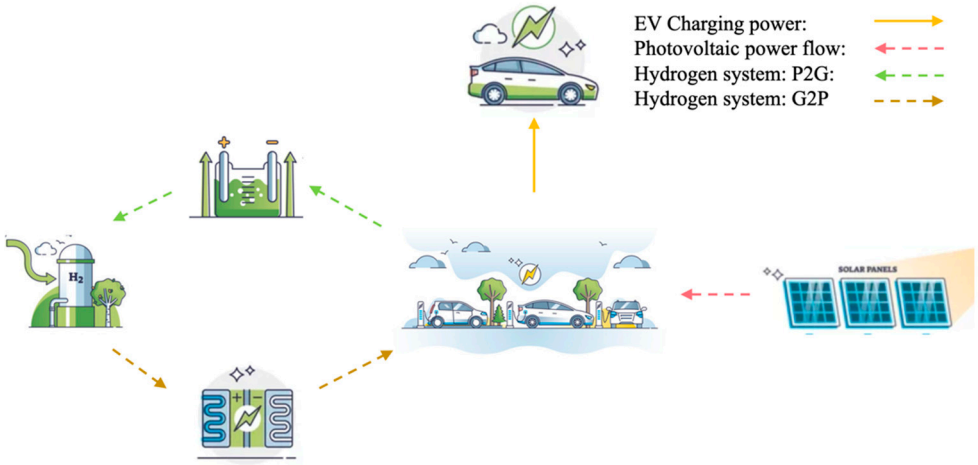

Figure 1. Single solar-hydrogen-storage-integrated electric vehicle charging station topology.

This paper mainly addresses the integration of renewable energy sources, energy management and optimization, and economic feasibility via game-theory-based P2P energy trading. The research focuses on the optimal sizing and integration of multiple renewable energy sources, including solar, hydrogen, and battery storage, within EV charging stations. This is crucial to maximize the utilization of renewable energy sources, minimize dependency on the grid, and ensure a sustainable and resilient energy supply. The combination of solar, hydrogen, and battery storage aims to leverage the complementary nature of these resources. Solar energy provides daytime power, hydrogen storage offers long-term energy storage, and batteries manage short-term fluctuations. This hybrid approach addresses the intermittent nature of renewable energy sources and improves the reliability and efficiency of the charging stations. This paper also develops advanced energy management strategies to optimize the operation of the SHS-EVCS. This includes the efficient allocation of energy resources, minimizing operational costs, and ensuring the reliability of the energy supply to

EVs. By focusing on the economic aspects, the research aims to make SHS-EVCSs financially viable, which involves exploring energy trading opportunities among charging stations.

2. Literature Review

Over the past few decades, policy-driven and technology-driven changes have played a significant role, which is also reflected in the development of charging infrastructure and electric vehicles. The concept of electric vehicles, which dates back to the early 20th century, was first introduced alongside internal combustion engines. However, electric vehicles struggled to compete due to scarce charging options and limited range [7,8]. Electric vehicles did not have a high degree of popularity, and by the end of the 20th century, people's interest in electric mobility was stimulated by advances in electric battery technology and environmental issues [9]. Judging from the development in recent years, the progress made by electric locomotives is very significant in terms of electric vehicle charging infrastructure, especially in the integration process of online personnel. The role played by wind and solar charging stations is becoming more common, and sustainable alternatives can be provided by conventional electricity.

MILP, on the other hand, offers a method for optimizing the power distribution in this P2P network, enabling the charging stations to make decisions that collectively enhance the system's performance. This mathematical approach helps determine the most efficient allocation of resources, minimizing costs and maximizing the utilization of renewable energy.

P2P energy trading is a revolutionary approach in the energy sector that allows individuals or businesses to buy and sell electricity directly with each other, typically without the involvement of traditional energy suppliers. This model leverages technology like blockchain and smart grids to facilitate these transactions. P2P energy trading can lead to more efficient use of renewable energy, lower energy costs, and reduced dependence on large-scale utility companies. It empowers consumers to become 'prosumers'—energy producers and consumers—and can contribute to a more sustainable energy system. Zhou's study [10] explores P2P energy sharing in smart communities, focusing on its role in advancing renewable energy adoption. It reviews P2P systems, addresses challenges, and examines artificial intelligence- and blockchain-based strategies for efficient energy trading, highlighting the potential economic and operational benefits [10]. The study emphasizes the need for further research to enhance P2P system effectiveness in renewable energy markets, particularly focusing on the dynamics of P2P energy trading in community microgrids. The research develops a game-theory-based decentralized trading scheme that focuses on the impact of distributed energy resource (DER) ownership [11]. P2P trading benefits participants economically but can lead to losses in communities with high photovoltaic penetration. It underscores the need for strategic DER management to optimize economic outcomes in P2P energy trading [8]. In [12], the authors employ fuzzy optimization techniques to balance economic and environmental objectives in energy trading and propose a multi-period P2P trading model that simultaneously minimizes electricity costs and carbon emissions. Another paper uses a distributionally robust optimization approach, utilizing a fuzzy set based on Wasserstein distance for renewable energy prediction error, and proposes a day-ahead microgrid P2P transactive energy trading model, employing a linear and convex programming approach to address the nonlinear aspects of the model [13]. A novel model for optimizing P2P energy trading in multi-microgrid systems uses Nash bargaining theory and data-driven chance constraints to manage uncertainties in renewable energy and load forecasting [14]. In [15], the authors provide a comprehensive analysis of 50 global peer-to-peer distributed renewable energy trading projects.

Game theory, a mathematical framework for analyzing strategic interactions among rational decision-makers, can be applied effectively in renewable energy trading. This application is particularly relevant in markets like P2P energy trading, where multiple participants (consumers, prosumers, utility companies) interact [16–18]. Game theory provides a framework for understanding the strategic interactions between independent

charging stations, each acting as rational players seeking to optimize their outcomes by modeling the decision-making processes of these entities, which can predict their behavior in response to varying energy supply, demand, and pricing conditions. In P2P energy trading, game theory can optimize energy distribution among participants. This involves strategies for energy distribution that are efficient, cost-effective, and fair, considering the varying production capacities and needs of different participants. In [16], the authors aimed to achieve higher economic income and maintain multi-agent income equilibrium. By employing the finite improvement property and a variable-step iterative convergence method, the study ensures efficient and accurate convergence of the model [16]. The model's simulation application demonstrates improved energy utilization rates and increased economic profits. The article [17] proposes a novel transactive energy market model using blockchain technology and game theory. The study introduces a proof-of-reserve consensus mechanism for prosumer–consumer transactions, enhancing energy trading efficiency and privacy, and uses game-theoretic market rules to establish a sustainable energy generation and consumption balance while ensuring economic agent privacy [17]. Another study [18] introduces a game-theory-based demand response program (DRP), integrating both incentive- and price-based DRP concepts, targeting residential, commercial, and industrial sectors; it evaluates three pricing strategies: fixed pricing, time-of-use pricing, and real-time pricing, along with their combinations. This approach leads to increased utility profits, reduced customer costs, and a more balanced load curve.

The fusion of game theory and MILP for designing and analyzing a P2P energy exchange system between multi-storage EV charging stations presents a novel solution that could revolutionize energy management in smart grids. This integrated approach addresses the economic aspects and contributes to the robustness and sustainability of energy systems in the era of decarbonization. This paper delves into such a system's complexities, exploring its potential to create a cooperative network that ensures energy security, fosters renewable integration, and paves the way for a greener future. It introduces a novel mixed-integer linear two-stage approach for analyzing the resiliency of power distribution systems. The study emphasizes the importance of considering both topological and electrical characteristics of distribution systems in resiliency analysis [19]. Study [20] introduces a MILP model optimized through a two-stage framework. This framework integrates system design with control problems of EV charging stations, using a design and analysis of a computer-experiments-based method [20]. Another study employs an iterative integer linear programming-based heuristic that efficiently tackles the multiple-choice knapsack problem with setup constraints [21]. This heuristic outperforms existing algorithms in solution quality and computation time, achieving optimal or near-optimal solutions for all tested instances. Linear programming and bi-objective optimization are particularly effective in long- and medium-term forecasts, reducing maximum errors significantly [22]. In Teng's paper [23], a distributed dual decomposition MILP-based energy management strategy for port-integrated energy systems is proposed to ensure reliable seaport operations.

Table 1 summarizes the model development and P2P using game theory. The paper [20] uses the CPLEX tool to solve the control problem of EVCSs. The study [24] uses several electricity sources to increase efficiency through game theory and P2P. Based on the previous studies, incorporating game theory into P2P systems involves using mathematical models to analyze and optimize interactions among participants with potentially conflicting interests. This approach is efficient in P2P networks, where decentralized entities negotiate, share resources, or trade without a central authority. Game theory provides a structured framework to model these interactions as strategic games, where each participant (player) seeks to maximize their utility through their actions [25–27].

Table 1. Literature review and benchmarking of relevant work.

Reference	Electricity Sources	Energy Exchange Applied	P2P or Game Theory Applied	Uses CPLEX Solver	Results
[20]	N/A	No	Yes	Yes	This approach utilizes a CPLEX solver tool to merge system design with control issues at EV charging stations, applying a method based on the design and analysis of computer experiments.
[28]	PV, grid	No	Yes	No	Using the suggested algorithm, prosumers enjoy increased earnings, while consumers experience reduced electricity expenses.
[29]	Grid, PV, wind	Yes	Yes	No	The suggested vehicle-to-vehicle market strategy enables EV owners to engage in peer-to-peer transactions, effectively lowering the cost of charging for individuals and evening out the demand on the power grid.
[30]	Grid	No	Yes	No	The proposed EV charging strategy optimally serves the individual interests of each EV, while also considering the demands of other EVs in the market for the next day.
[31]	Battery, PV	Yes	Yes	No	The method that this article proposed can significantly bolster resilience by up to 80% and extend battery lifespan by 32–37%.
[24]	Battery storage, PV, grid	Yes	Yes	No	The outcomes of the proposed strategy demonstrate an enhancement in energy utilization efficiency by considering the effects of the power system within peer-to-peer energy trading scenarios.
[32]	PV, wind, energy storage system, grid	No	Yes	No	This research demonstrates that the suggested control strategy provides a viable and practical method for managing an autonomous distributed system as miniature microgrids within the context of the electricity market, considering the competitive, non-cooperative relationships among microgrids.

Table 1. *Cont.*

Reference	Electricity Sources	Energy Exchange Applied	P2P or Game Theory Applied	Uses CPLEX Solver	Results
[33]	PV, storage system (heating, cooling, and battery), grid	Yes	Yes	No	The model offers a pragmatic and effective means for assisting in the determination of equitable trading prices, while also furnishing valuable perspectives on the optimal design of energy infrastructures.
[34]	PV, wind, energy storage system	No	Yes	No	The market simulation employs a non-model-based, game theory approach, wherein participants adjust their strategies based on the expected returns measured from the market.
[35]	PV, battery energy storage, hydrogen storage, grid	Yes	No	No	This holistic strategy for energy optimization allows the station to accommodate the variable energy needs for charging electric vehicles, thereby reducing costs, and enhancing sustainability.
This work	PV, battery energy storage, hydrogen storage, grid	Yes	Yes	Yes	The method not only boosts SHS-EVCS revenue through P2P transactions but also helps manage operational and maintenance expenses, contributing to the growth of the renewable energy sector.

The specific contributions of this work are as follows:

- Proposal of a P2P optimal dispatch strategy rooted in game theory for SHS-EVCS, aimed at achieving greater economic returns by ensuring income equilibrium across multiple SHS-EVCSs.
- Design and implementation of a CPLEX solver specifically to solve the linear-based simulation, predominantly employed for addressing locational queries. This solver is resolved and subsequently integrated with an SHS-EVCHs model to enhance its applicability.
- This study examines the synergistic collaborations and operational dynamics among diverse stakeholders to elucidate the shared economic benefits, with a particular emphasis on methodologies reliant on SHS-EVSC for the facilitation of energy sharing and the optimization of economic dispatch.

3. Problem Formulation

3.1. Objective Function

To reduce anticipated costs, the objective function F of SHS-EVCS includes the cost of hydrogen energy storage, gas turbine costs, solar energy costs, grid costs, battery storage costs, and P2P costs, minus the revenue from selling electricity (1).

$$F = min\sum_{n\in N}^{1} F_n = min\sum_{n}^{N}\sum_{t}^{T}\left(C_{n,t}^{E_H} + C_{n,t}^{FC} + C_{n,t}^{grid} + C_{n,t}^{Pv} + C_{n,t}^{p2p} + C_{t}^{Bes} - C_{n,t}^{sell}\right) \quad (1)$$

where

$C_{n,t}^{E_H}$ is hydrogen cost;

$C_{n,t}^{FC}$ is fuel cell generator cost;
$C_{n,t}^{grid}$ is grid cost;
$C_{n,t}^{Pv}$ is solar cost;
$C_{n,t}^{p2p}$ is p2p trading cost;
C_{t}^{Bes} is battery energy storage;
$C_{n,t}^{sell}$ is sale revenue.

3.2. Hydrogen System Model

3.2.1. Electrolyzer Model

The water electrolysis hydrogen production process uses water as raw material, and its composition mainly includes devices such as the electrolyzer, hydrogen (oxygen) gas–liquid–solid separators, hydrogen (oxygen) gas coolers, and hydrogen (oxygen) gas purifiers [36]. Using water decomposition to produce hydrogen is an efficient, environmentally friendly, and convenient new method for hydrogen production. The mathematical model of the electrolyzer for hydrogen production adopted in this paper is shown in Equation (2):

$$E_{AE,t} = \frac{v}{a} P_{AE.t} \tag{2}$$

$P_{AE.t}$ and $E_{AE,t}$ represent the electrical power consumed and the quantity of hydrogen produced by the electrolyzer, respectively. ν denotes the conversion efficiency, which is 75%, and a represents the conversion coefficient for electric energy to the equivalent energy in hydrogen, valued at 39.65 kWh/kg [37].

3.2.2. Fuel Cell Generator Model

Hydrogen fuel cells, as an energy conversion device within the system, are an important part of hydrogen energy applications. Hydrogen fuel cells differ from dry cells and batteries, which are types of energy storage devices that store energy and release it where needed [38]. Strictly speaking, hydrogen fuel cells are not energy storage devices but rather devices that can generate electricity through the chemical properties of hydrogen and oxygen. Their basic principle is the reversible reaction of water electrolysis. This paper focuses on the process of the battery generating electrical energy by consuming hydrogen. Therefore, the mathematical expression for the hydrogen fuel cell adopted in this article is shown as Equation (3):

$$P_{FC} = \eta_{FC} a E_{FC} \tag{3}$$

P_{FC} and E_{FC} represent the output power and the quantity of hydrogen consumed by the fuel cell, respectively. η_{FC} is the energy conversion efficiency, which is 70% [37].

3.2.3. Hydrogen Storage Tank Model

Hydrogen storage tanks [39], as devices for storing hydrogen, come in different types based on various hydrogen storage technologies. The technology currently used most is high-pressure gaseous hydrogen storage. The storage tanks used in this technology are mainly made of conventional stainless acid-resistant steel plates and aluminum alloys. The process technology for their design and production is relatively mature, with low cost, a rapid rate of gas charging and discharging, and the capability to store hydrogen at normal temperatures. The mathematical model for the high-pressure hydrogen storage tanks used in this paper can be represented by Equation (4):

$$E_{hs}(t) = (1 - \delta_{hs}) E_{hs}(t-1) + \left[E_{hs}^{in}(t) \eta_{hs}^{in} - \frac{E_{hs}^{out}(t)}{\eta_{hs}^{out}} \right] \Delta t \tag{4}$$

$E_{hs}(t-1)$ and $E_{hs}(t)$ represent the total quantity of hydrogen stored in the hydrogen tank at time $t-1$ and t, respectively; δ denotes the energy storage decay rate of the hydrogen tank, which is 0.05; $P_{hs}^{in}(t)$ represents the input quantity of hydrogen into the

hydrogen tank; $P_{hs}^{out}(t)$ represents the output quantity of hydrogen from the hydrogen tank; η_{hs}^{in} is the input efficiency of the hydrogen tank, which is 0.98; and η_{hs}^{out} is the output efficiency of the hydrogen tank, also 0.98 [35].

3.3. Photovoltaic Model

Based on the photovoltaic effect, the PV cells in a PV power generation system can utilize sunlight to produce electrical energy. The power generation efficiency model is given as Equation (5):

$$P_{pv} = P_{STC} G_{AC} \frac{[1 + k(T_c - T_r)]}{G_{STC}} \tag{5}$$

k is the power temperature coefficient, valued at -0.45; different photovoltaic components will have different values, generally taken as $-0.3\%/^{\circ}\mathrm{C}$; and P_{STC} is the rated output power of the PV components under standard test conditions. G_{AC} is the real-time solar irradiance intensity where the photovoltaic cell operates; T_c is the real-time temperature of the photovoltaic component surface; G_{STC} is the illumination under standard test conditions, valued at 1000 W/m^2; and T_r is 25 °C.

$$T_C = T_a + \frac{G_C}{800}(T_N - 20) \tag{6}$$

T_a is the ambient temperature, and T_N is the rated temperature at which the photovoltaic cell operates.

3.4. Battery Energy Storage Model

Batteries can effectively smooth out fluctuations caused by sudden changes in load demand within a microgrid. When the output power of photovoltaics exceeds the load demand power, the battery is in a charging state; conversely, when the output power is less than the load demand power, the battery is in a discharging state. Its characteristics are shown in (7) and (8).

Discharging model:

$$E_{BSS}(c) = E_{BSS}(c-1) + [E_{gen}(c) - \left(\frac{E_{load}(c)}{e_{inv}}\right)]\eta_b^{dch} \tag{7}$$

Charging model:

$$E_{BSS}(c) = E_{BSS}(c-1) - [E_{gen}(c) - \left(\frac{E_{load}(c)}{e_{inv}}\right)]/\eta_b^{ch} \tag{8}$$

where $E_{BSS}(c)$ is the energy of the battery at the c-th time, $E_{gen}(c)$ is the energy generated by the generator at the c-th time, $E_{load}(c)$ is the energy of the load at the c-th time, e_{inv} is the efficiency of the inverter, valued at 95%, and η_b^{ch} and η_b^{dch} represent the charging and discharging efficiency of the battery, both valued at 80% [40].

3.5. P2P Trading Model

3.5.1. P2P Internal Trading Revenue [13]

$$C_{n,t}^{sell} = \rho_{n,t}^{inter} P_{n,t}^{load} \tag{9}$$

$\rho_{n,t}^{inter}$ is the price of number n SHS-EVCSs selling electricity to other SHS-EVCSs using internal load.

3.5.2. P2G Trading with Grid

$$C_{n,t}^{grid} = \rho_{n,t}^{B} P_{n,t}^{B} - \rho_{n,t}^{g} P_{n,t}^{g} \tag{10}$$

$\rho^B_{n,t}$and $P^B_{n,t}$ are the price and electricity purchased by SHS-EVCS n from shared battery energy storage at time t. $\rho^g_{n,t}$ and $P^g_{n,t}$ are the price and power sold to the grid. Usually, $\rho^g_{n,t}$ is much lower than $\rho^B_{n,t}$, which can increase the profits or reduce costs through P2P trading.

3.5.3. P2P Transaction Energy Trading Cost

$$C^{p2p}_{n,t} = \sum\nolimits^{1}_{i \in N \backslash n} \rho^i_{n,t} P^i_{n,t} \tag{11}$$

where N is the set of charging stations participating in P2P trading. $\rho^i_{n,t}$ is the transaction price between SHS-EVCS n and SHS-EVCS N at time t.

3.5.4. P2P Transactive Energy Trading Constraints

For any time, the electricity sold and purchased should be balanced.

$$P^i_{n,t} = -P^n_{i,t}, \forall t \in T, \forall n \in N, i \in N \backslash n \tag{12}$$

3.6. Game Theory Model

Cooperative game theory [41] is a branch of game theory that focuses on understanding the behavior and strategies of groups of players who can form coalitions and collaborate to achieve better outcomes than they might individually. Unlike non-cooperative game theory, where the emphasis is on individual players' strategies and equilibria, cooperative game theory examines how groups of players can work together and how the collective benefits can be distributed among them. Key elements include the characteristic function, which defines the potential payoff for any coalition, and solution concepts like the Core, the Shapley Value, and the Nash Bargaining Solution, which help determine fair ways to distribute the collective payoff among the members.

Gamer: N(SHS-EVCS1(1), SHS-EVCS2, SHS-EVCS3. . . SHS-EVCSN)

Strategy: electricity prices (ρ); power transaction value set (P)

Matrix:

$\rho = \left[\rho^{cs}_{1,1} \ldots \rho^{cs}_{N,t} \ldots \rho^{cs}_{n,t} \ldots \rho^{cs}_{N,t} \ldots \rho^{cs}_{N,T}\right]$ All gamers' pricing at different times.

$P = \left[P^{cs}_{1,1} \ldots P^{cs}_{N,t} \ldots P^{cs}_{n,t} \ldots P^{cs}_{N,t} \ldots P^{cs}_{N,T}\right]$ All gamers' transaction value.

Benefits: $U = \left[U^{cs}_{1,1} \ldots U^{cs}_{N,1} \ldots U^{cs}_{n,t} \ldots U^{cs}_{N,t} \ldots U^{cs}_{N,T}\right]$ Benefit set matrix consisting of the benefits of purchasing and selling electricity at different times for all players in the game.

Buyer: if there is energy exchange between charging stations, and the upper limit is $E^g_{n,t}$ (electricity buying from grid), then $\left|E^{cs}_{n,t}\right| \leq E^g_{n,t}$; the SHS-EVCS is called a buyer at time t.

Seller: if there is energy exchange between charging stations, and the upper limit is $E^{g*}_{n,t}$ (electricity selling to grid), then $E^{cs}_{n,t} \leq E^{g*}_{n,t}$; the SHS-EVCS is called a seller at time t.

When $SHS - EVCS_n \in Sellers$, the benefits at time t are

$$U^{cs}_{n,t} = \rho^{cs}_{n,t} P^{cs}_{n,t} \Delta t + \rho^g_{n,t}\left(E^{g*}_{n,t} - E^{cs}_{n,t}\right)\Delta t = \sum\nolimits_{i \in buyers} \rho^{cs}_{n,t} E^{cs}_{ni,t} \Delta t + \rho^g_{n,t}\left(E^{g*}_{n,t} - \sum\nolimits_{i \in buyers} E^{cs}_{ni,t}\right)\Delta t \tag{13}$$

When $SHS - EVCS_n \in Buyers$, the benefits at time t is:

$$U^{cs}_{i,t} = \sum\nolimits_{n \in sellers} \rho^{cs}_{n,t} E^{cs}_{in,t} \Delta t + \rho^{g*}_{n,t}\left(E^g_{n,t} - \sum\nolimits_{n \in sellers}\left|E^{cs}_{in,t}\right|\right)\Delta t \tag{14}$$

where $P^{cs}_{in,t}$ means *SHS-EVCS i* follows the *SHS-EVCS n* pricing rule $\rho^{cs}_{n,t}$ to buy the power at time t, $E^{cs}_{in,t} < 0$

3.7. Model Constraints

3.7.1. Hydrogen Constraints

- Electrolyzer Constraint:

$$u_{hs}(t)E^{o}_{hs,min} \le E^{o}_{ae}(t) \le u_{hs}(t)E^{o}_{hs,max} \tag{15}$$

where $E^{o}_{hs,min}$ is the lower output limit of the electrolyzer, $E^{o}_{hs,max}$ is the upper output limit of the electrolyzer, and $u_{hs}(t)$ is the state variable of the electrolyzer.

- Hydrogen tank constraints:

$$\begin{cases} u^{in}_{hs}(t)E^{in}_{hs,min} \le E^{in}_{hs}(t) \le u^{in}_{hs}(t)E^{in}_{hs,max} \\ u^{out}_{hs}(t)E^{out}_{hs,min} \le E^{out}_{hs}(t) \le u^{out}_{hs}(t)E^{out}_{hs,max} \\ E_{hs,min} \le E_{hs}(t) \le E_{hs,max} \\ u^{in}_{hs}(t) + u^{out}_{hs}(t) \le 1 \end{cases} \tag{16}$$

where $E^{in}_{hs,min}$ is the lower intput limit of the electrolyzer, $E^{in}_{hs,max}$ is the upper input limit of the electrolyzer, u^{in}_{hs} is the hydrogen tank storage state variable, and u^{out}_{hs} is the hydrogen tank release state variable.

- Fuel cell generator constraint:

$$0 \le P^{out}_{FC}(t) \le P^{out}_{FC,max} \tag{17}$$

where $P^{out}_{FC,max}$ is the maximum power output for the fuel cell generator.

3.7.2. Photovoltaic Constraint

$$P_{pv,\ min} < P_{PV}(t) < P_{pv,\ max} \tag{18}$$

where $P_{pv,min}$ and $P_{pv,max}$ are the minimum and maximum PV power output.

3.7.3. Battery Storage Constraint

$$E^{min}_{BSS} \le E_{BSS,j}(k) \le E^{max}_{BSS} \tag{19}$$

$$\begin{cases} E^{min}_{BSS} = (1 - DOD)E^{max}_{BSS} \\ E^{max}_{BSS} = N_{BSS}E_{rate\_BSS} \end{cases} \tag{20}$$

where E_{rate_BSS} is the self-discharge rate of the battery, and DOD is the depth of discharge, valued at 90%.

4. Case Study

Figure 2 provides a detailed schematic representation of four SHS-EVCSs engaged in energy exchange. The illustration uses a yellow line to denote the process of EV charging. The light blue bidirectional arrows symbolize the dynamic transactions of buying and selling electricity between the EVCSs, shared storage facilities, and the grid. Green dashed lines within the hydrogen storage system delineate the conversion of electrical power into gas via the electrolyzer, while the dark yellow dashed lines indicate the reconversion of gas back into electricity through the fuel cell generator. Additionally, pink dashed lines associated with the solar arrays illustrate photovoltaic power generation. A notable feature of this system is represented by the blue double-arrow line, which indicates the comprehensive energy exchanges occurring among the four SHS-EVCSs.

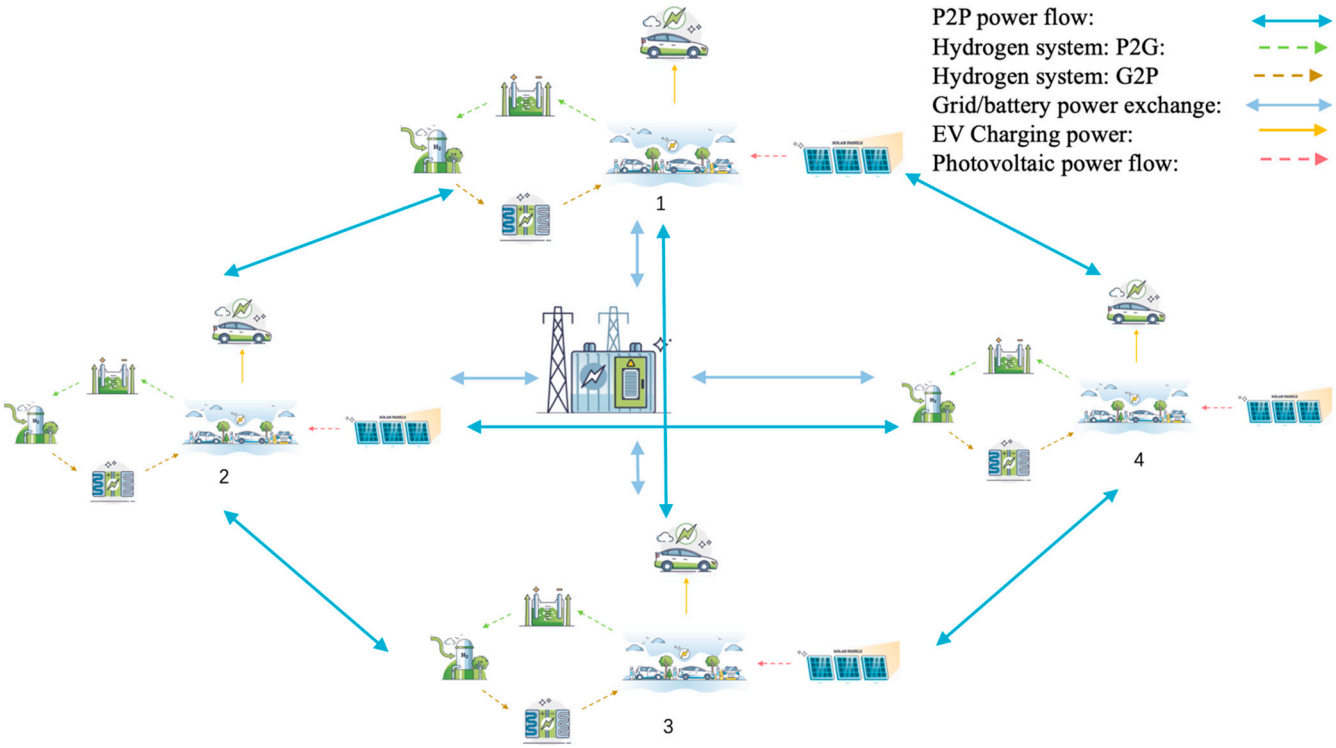

Figure 2. Topology of multi-SHS-EVCSs.

In the methodology simulation, Tables 2 and 3 detail the technical and economic parameters for four SHS-EVCSs, providing a comprehensive overview of each station's operational capabilities and financial aspects. These parameters include, but are not limited to, energy production capacities, operational efficiencies, maintenance and operational costs, and potential revenue streams. Table 4 presents a set of design variables crucial for the simulation process. These variables are instrumental in modeling the performance and economic viability of the stations under different scenarios, including energy demand fluctuations, market price variations, and changes in operational conditions.

Table 2. Technical parameters of SHS-EVCSs in four Dali boroughs [27,34,39].

Parameters	Longzu 1 (EVCS1)	Longzu 2 (EVCS2)	Qiliqiao (EVCS3)	Fuyuan (EVCS4)
Charger capacity (kW)	360	360	360	360
Number of chargers per station	10	10	12	8
PV installed capacity(kW)	1500	1500	2000	1000
Shared battery capacity (kWh)	10,000	10,000	10,000	10,000
Hydrogen tank capacity (m^3)	2000	2000	3000	1500
Fuel cell generator capacity (kW)	800	800	1000	600
Battery initial state of charge (%)	40	40	40	40
Minimum battery state of charge (%)	25	25	25	25
Maximum battery state of charge (%)	100	100	100	100
Battery charge and discharge efficiency (%)	80	80	80	80
Initial capacity of gas tank (%)	30	30	30	30
Tank storage efficiency (%)	98	98	98	98
Energy-to-gas efficiency (%)	70	70	70	70
Electricity-to-gas coefficient (kWh/m^3)	0.2	0.2	0.2	0.2
Hydrogen conversion efficiency (%)	75	75	75	75
Gas-to-electricity coefficient (m^3/kWh)	0.295	0.295	0.295	0.295

Table 3. Economic parameters of SHS-EVCSs in four Dali boroughs [42–44].

Parameters	Longzu 1	Longzu 2	Qiliqiao	Fuyuan
PV capital cost (GBP/kW)	286	286	286	286
Battery capital cost (GBP/kWh)	39.6	39.6	39.6	39.6
Hydrogen tank cost (GBP/m^3)	7.5	7.5	7.5	7.5

Table 4. Design variables for SHS-EVCSs [35,36,40].

Input	Technical Specification
PV output power [kW]	$P_{STC} G_{AC} \frac{[1+k(T_c-T_r)]}{G_{STC}}$
Hydrogen output power [kW]	$E^{t-1}_{H_2,i} - \left(P^t_{H-FC,i} + P^t_{SH,i} + P^t_{H_2,i}\right)\Delta t$
Battery output power [kW]	$P_{Bat,e,t1}(1-\sigma_{Bat,e}) + \left(P^{cha}_{Bat,e,t} * \eta^{cha}_{Bat,e} + \frac{P^{dis}_{Bat,e,t}}{\eta^{dis}_{Bat,e}}\right)$

Dali, located in Yunnan Province, China, was chosen as the case study primarily due to its geographic features and the prosperity of its tourism sector. Surrounded by mountains and lakes, Figure 3 shows that Dali's transportation is heavily dependent on two main north–south highways, and the constant tourism demand throughout the year further exacerbates transportation needs. Therefore, constructing charging stations has become a key measure to optimize the transportation infrastructure and support sustainable development. This not only helps alleviate traffic pressure but also encourages the use of eco-friendly transportation methods, such as electric vehicles, thereby enhancing Dali's tourism experience and environmental protection levels. There are numerous charging points in the parking area, but most require both parking and charging fees, which can be inconvenient for users. SHS-EVCSs offer a more cost-effective solution for electric vehicle owners. Additionally, SHS-EVCSs prioritize providing a safer and more secure charging environment, ensuring peace of mind for all EV drivers.

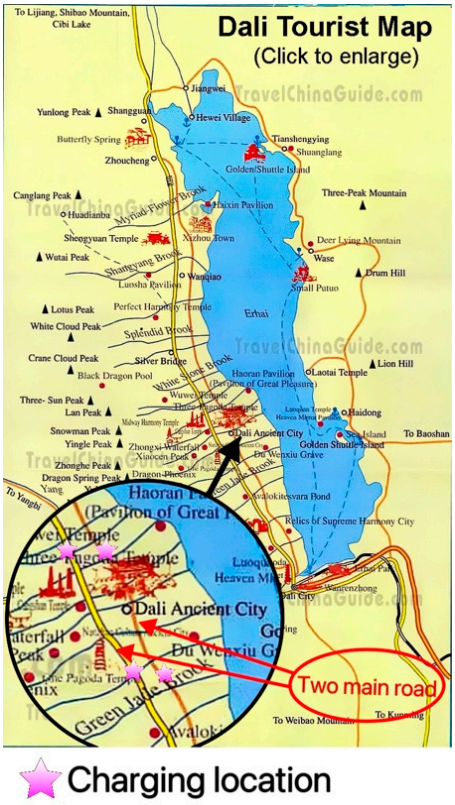

Figure 3. Topology of 2 main roads in Dali.

In the cooperative game model within the SHS-EVCS P2P trading framework, each EVCS functions as both a producer and a consumer, indicating that multiple entities reach a consensus. Therefore, the game-theory-based P2P process, as depicted in Figures 5–15, follows these steps and Figure 4 shows the game-theory-based P2P flow chart:

(a) Initiate trading.
(b) All SHS-EVCSs request energy exchanges.
(c) Aim to maximize the coalition's profits. Analyze each EVCS's energy trading needs to determine if they meet the model's constraints during the specified time (ensuring optimal profit for the coalition at time t), and then calculate the energy trading plan.
(d) Confirm the energy trading flow and calculate profits.
(e) If the profit maximizes the coalition's benefits, proceed to step (f); if not, return to step (c) and recalculate the energy exchange quantities.
(f) Allocate profits based on the constraints.
(g) Conclude the energy trading.

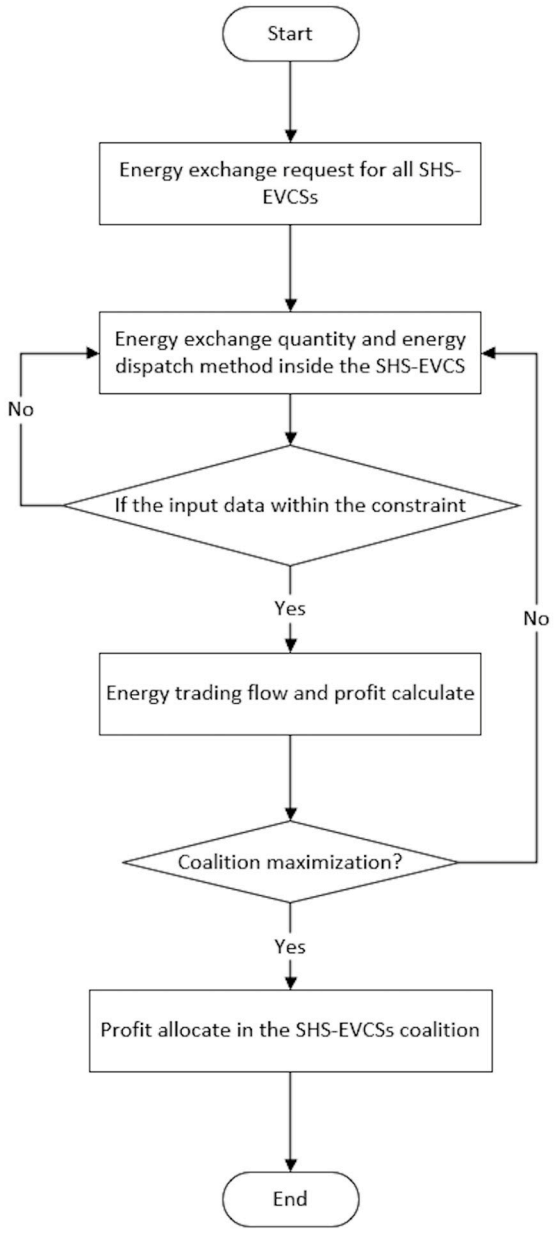

Figure 4. Game-theory-based P2P flow chart.

5. Results and Discussion

Figure 5 provides a detailed depiction of the variation in grid electricity prices and internal electricity trading prices over time. Grid electricity price remains essentially stable at 0.018 GBP/kWh until after 8 a.m., where it rises slightly to 0.05 GBP/kWh. This reflects the base price of the grid or time-specific tariff adjustments. The internal electricity purchase price briefly rises to 0.048 GBP/kWh around 7 a.m., then rises again around 0.075 GBP/kWh at 11, maintaining this level until 1 p.m. After 6 p.m., the purchase price rises once again to 0.075 GBP/kWh and continues until it starts to decline after 8 p.m. The internal electricity sale price rises to about 0.47 GBP/kWh around 7 a.m., then rises around 11 a.m., and drops again at 2 p.m., inversely mirroring the purchase price movements. After 6 p.m., the sale price sharply rises to 0.75 GBP/kWh, remaining at this level until it starts to decline after 8 p.m. These price fluctuations reflect changes in supply and demand within the internal market or adjustments in electricity trading strategies. Price increases represent an increase in demand or a decrease in supply, while decreases indicate a reduction in demand or an increase in supply. The disparity between the internal purchase and sale prices represents the margin for trading profits or opportunities for cost recovery.

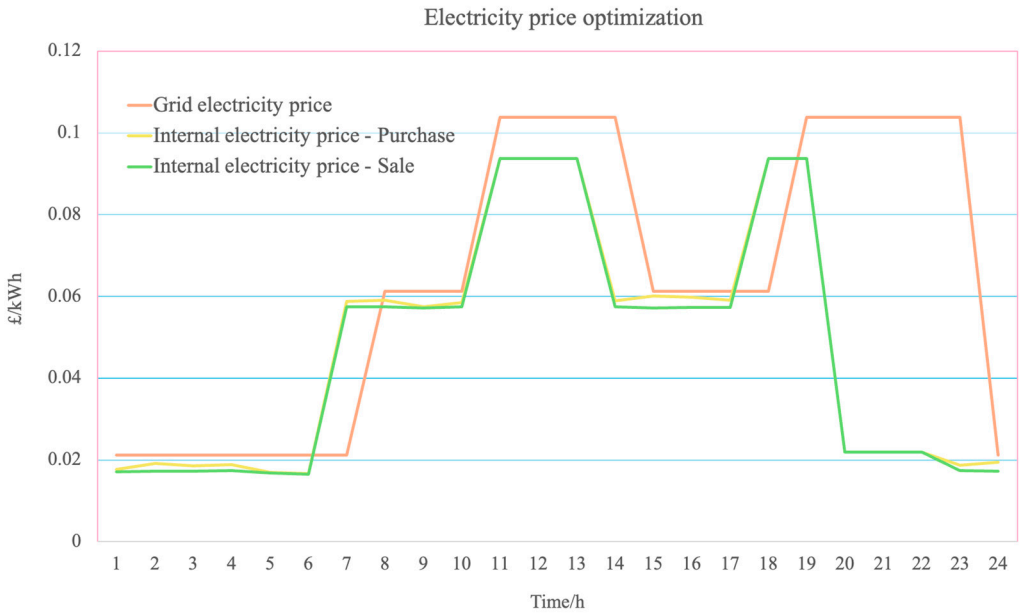

Figure 5. Electricity price optimization.

Figure 6 shows the number of electric vehicles for each charging station after optimization on different days. During the weekend, SHS-EVCS 1 shows an initial decrease after 2 a.m., followed by a slight drop after 6 a.m. A significant decrease is observed after 1 p.m., when the number of charges drops sharply. SHS-EVCS 2 exhibits that at 1 p.m., the first 25 cars charge in this station. At 8 p.m., 11 p.m., and 12 a.m., there are only 25 cars at each time. For SHS-EVCS 3, there are only 26 drivers who charge their cars at 6 p.m. SHS-EVCS 4, which has the most equal charging number for 24 h, only increased the charging number at 11 p.m. During weekdays, all EVCSs particularly show significant activity peaks around 9 a.m. and 10, correlating with typical commuting times. EVCS2 is the most utilized, suggesting higher demand or more frequent use compared to the others. All stations exhibit minimal activity during the early morning, which is before 6 a.m. This figure displays the traffic flow optimization results for four SHS-EVCSs. When designing this simulation model, multiple factors were considered, including geographical constraints, traffic control measures, and energy exchange. Through the analysis of these factors, the simulation model provided an optimal traffic flow management strategy. The increase and decrease indicated in the figure refer to the traffic flow adjustments at each charging station under specific conditions based on the optimal solutions derived from

the simulation outputs. By adjusting traffic flows, we can more effectively distribute and utilize charging resources, thus addressing potential congestion issues during the electric vehicle charging process. Overall, this figure provides a comprehensive plan on how to optimally manage and schedule vehicle access to charging stations, ensuring charging efficiency while also enhancing the user's charging experience. Overall, this information is valuable for future research to optimize operations, perhaps by reducing power supply or staffing during low-demand hours.

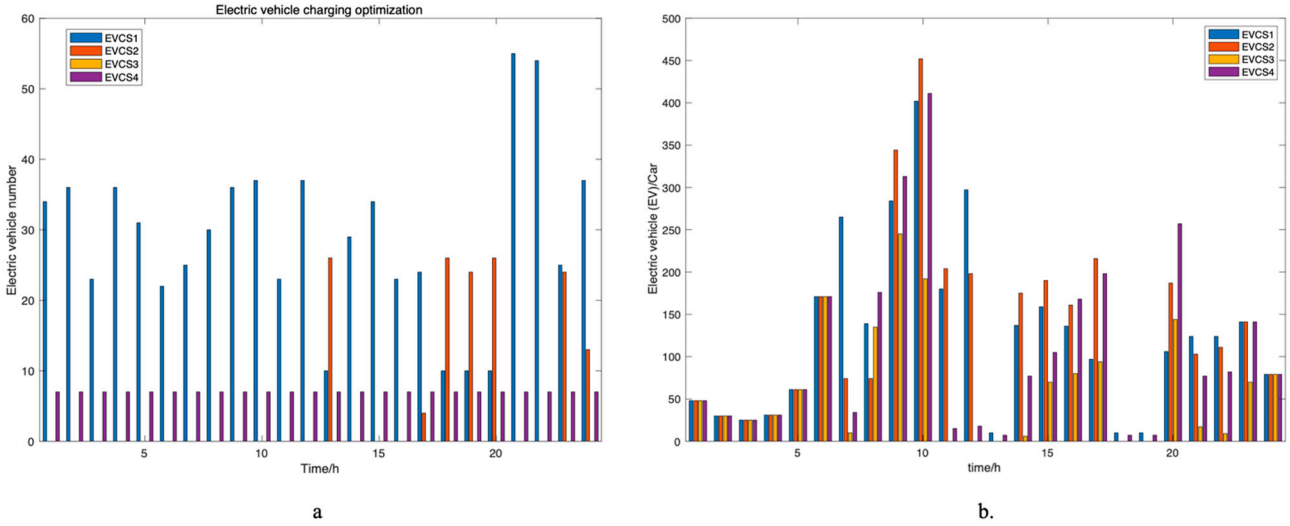

Figure 6. Optimization of the number of electric vehicle charging stations: (**a**) weekend; (**b**) weekday.

Figures 7–10 delineate the energy utilization and electricity load profiles of four distinct SHS-EVCSs. During the daytime, photovoltaic generation emerges as the predominant source of electricity, harnessing solar irradiance. Figures 9 and 10 show similar trends in energy consumption and electrical load, attributable to their analogous locational contexts, predominantly residential in nature. After sunset, the reliance transitions to hydrogen fuel cells for electricity generation, supplemented by acquisitions of electricity from a communal battery storage system. This shift underscores the versatility of the integrated energy systems within the SHS-EVCS framework.

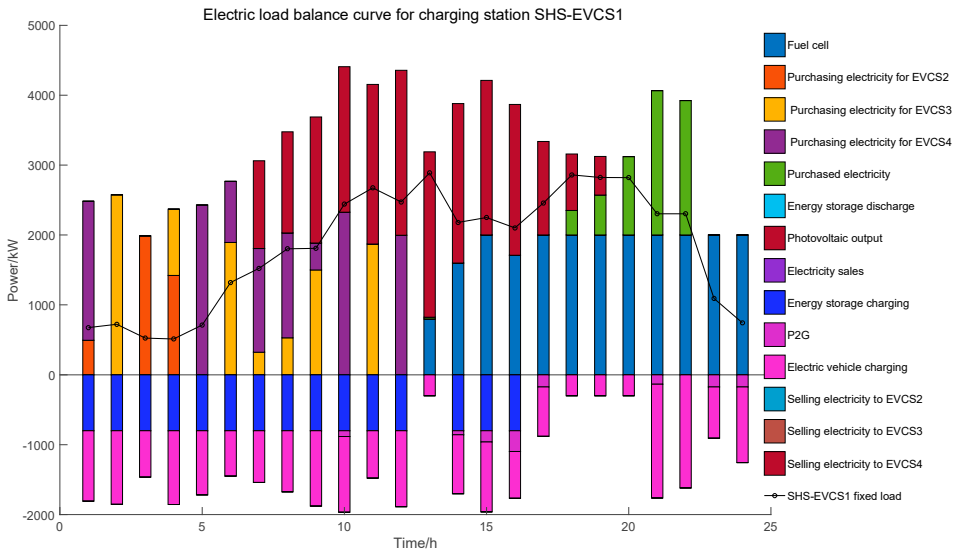

Figure 7. SHS-EVCS1 renewable energy usage and electricity load curve.

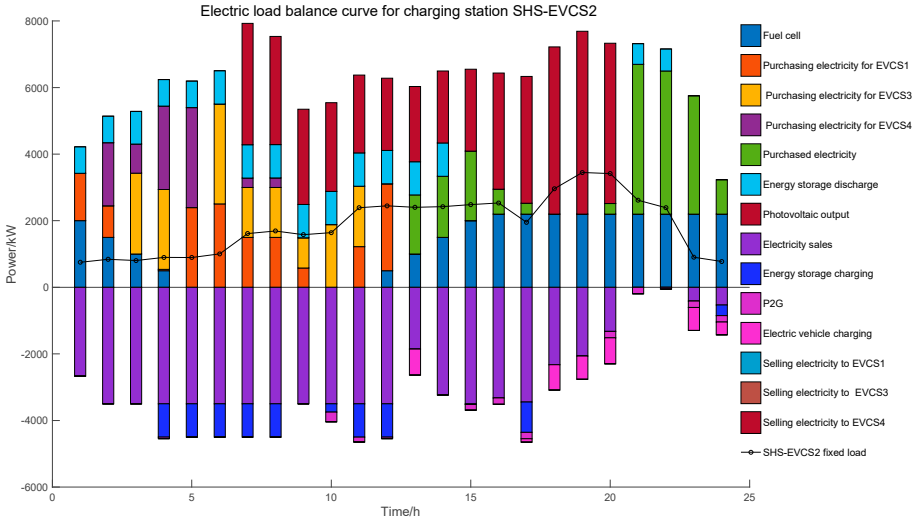

Figure 8. SHS-EVCS2 renewable energy usage and electricity load curve.

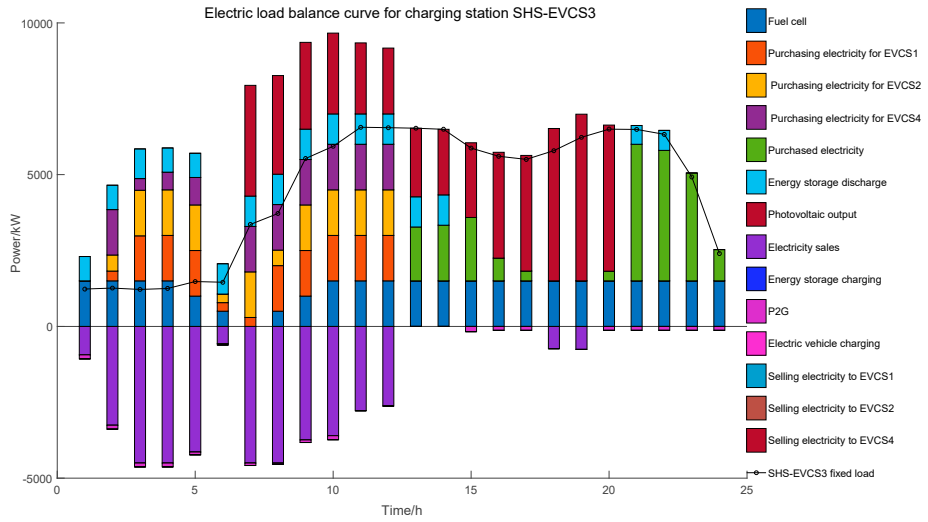

Figure 9. SHS-EVCS3 renewable energy usage and electricity load curve.

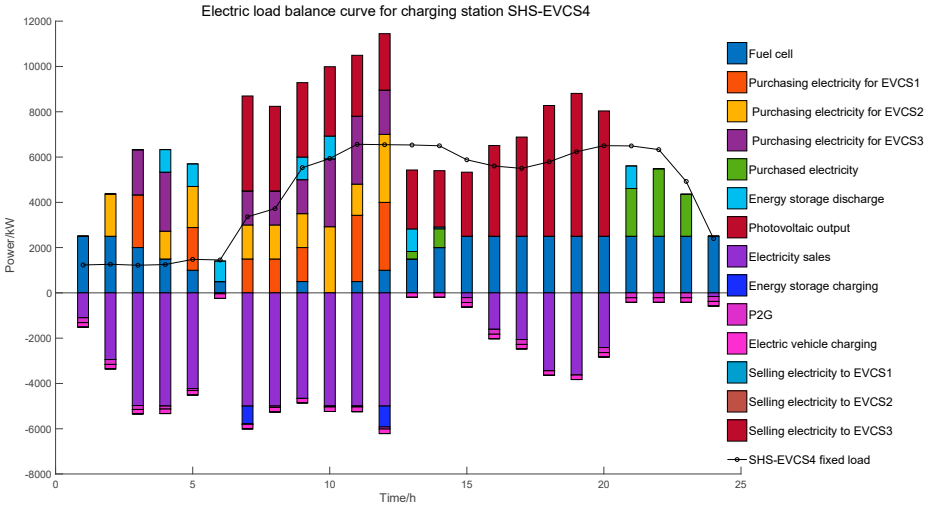

Figure 10. SHS-EVCS4 renewable energy usage and electricity load curve.

Additionally, these infrastructures engage in inter-station power trading, exemplifying the benefits of a decentralized energy network. Optimizing the energy management strategies shown in these figures can lead to the best possible economic benefits while also reducing infrastructure costs. This optimization improves how efficiently each SHS-EVCS operates and makes the power grid more sustainable by using different types of energy storage and generation. Managing energy in this strategic way is key to developing robust, smart power grids and moving toward being able to produce energy independently.

Figure 11 presents a composite graph combining a bar figure and a line graph, illustrating the operational dynamics of an energy storage system over a 24 h period. For the bar figure, positive values represent charging power, indicating the periods when the energy storage system is actively storing energy. Negative values represent discharging power, showing when the system is delivering energy back to four SHS-EVCSs. Notably, during weekends, the charging activities peak around 1 a.m., 6 a.m., 9 a.m., 10 a.m., 1 p.m., 2 p.m., 8 p.m.–10 p.m., possibly correlating with off-peak hours or periods of surplus energy production when travel is less constrained. Discharge events are more sporadic, with significant outputs observed around 7 a.m., 8 a.m., 11 a.m., 12 p.m., 3 p.m.–5 p.m., and 12 a.m., likely aligning with peak demand periods or the operational needs for grid stability. During weekdays, the energy storage undergoes intense charging activities, notably at 4 a.m., 5 a.m., 11 a.m., 12 p.m., 6 p.m., and 7 p.m. The graph highlights these occurrences with blue bars, which correspond to peaks in the battery's state of charge, depicted as red circles on the line graph. This pattern corroborates the anticipated behavior of the battery storage system within the SHS-EVCS framework, efficiently aligning charging and discharging activities with the fluctuations in energy demand and supply dynamics.

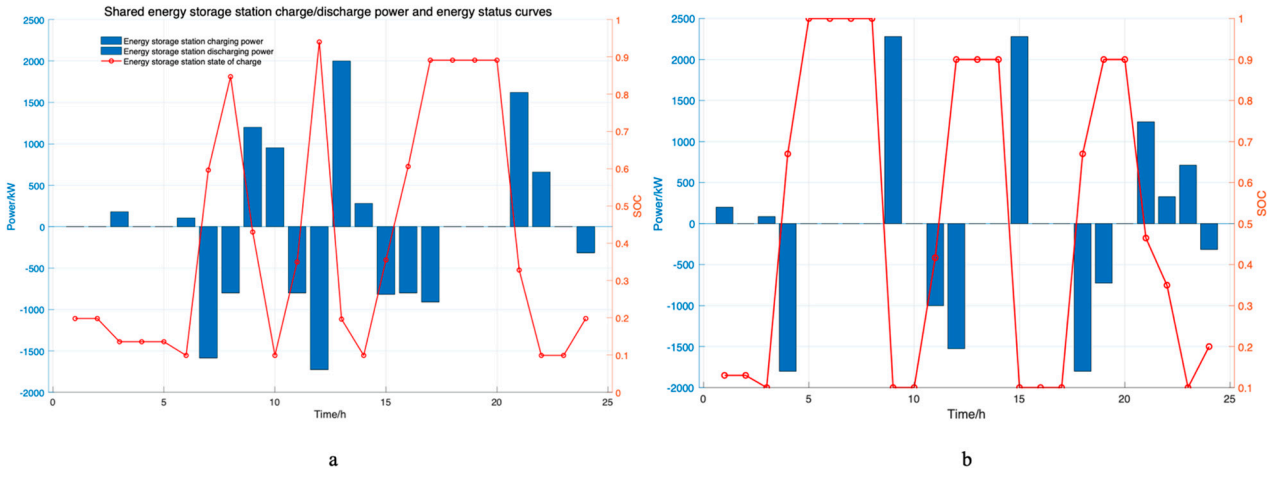

Figure 11. Battery storage power flow and State of Charge (SOC): (**a**) weekends; (**b**) weekdays.

In the observed data, the state of charge (SOC) of the energy storage system exhibits a cyclic behavior characterized by declines during periods of positive bar representation and increases when the bars are negative. This pattern indicates the regular charging and discharging cycles that the system undergoes. The SOC reaches peak levels at various intervals over a 24 h cycle, aligning with the strategic operational practice of charging during periods of low energy demand and discharging during peak demand periods or when the energy generation is insufficient. Additionally, discharging is implemented when purchasing electricity from the grid or shared battery systems is economically disadvantageous due to higher prices. This cyclical pattern of SOC fluctuations is demonstrative of an effectively managed energy storage system that is dynamically adjusting its charge and discharge cycles. Such management is crucial for leveraging fluctuations in energy prices, enhancing the utilization of generated renewable energy, and thereby increasing the overall stability and efficiency of the SHS-EVCSs. This active modulation not only supports the

economic operation within the energy market but also plays a significant role in stabilizing the grid and ensuring a reliable supply of green energy.

Figure 12 shows the diurnal consumption patterns of hydrogen across four SHS-EVCSs. An examination of the hourly data reveals distinct temporal variations in hydrogen utilization. In the early morning hours, from midnight to 10 a.m., CS 1 demonstrates a consistent level of usage, while CS 2 experiences a modest uptick. Conversely, CS 3 and 4 show a decline in usage, with CS 3 encountering a notably sharper fall. After 10 a.m., a significant rise in hydrogen use at CS 3 indicates an increase in operational activities or demand. The remaining charging stations—CS 1, CS 2, and CS 4—also see minor rises in their usage. Until 5 p.m., there's a pronounced increase across all SHS-EVCSs, signaling elevated demand or heightened charging activities. CS 1 registers the largest increase, succeeded by CS 2, CS 4, and CS 3. In the late evening hours, from 10 p.m. to midnight, all stations' activities level off, reaching a steady state of demand. The consumption pattern appears to mirror conventional daily usage trends, characterized by a trough in the early dawn hours and a crest during the evening. These fluctuations are likely reflective of habitual consumer charging behaviors or inherent operational cycles of the SHS-EVCS network.

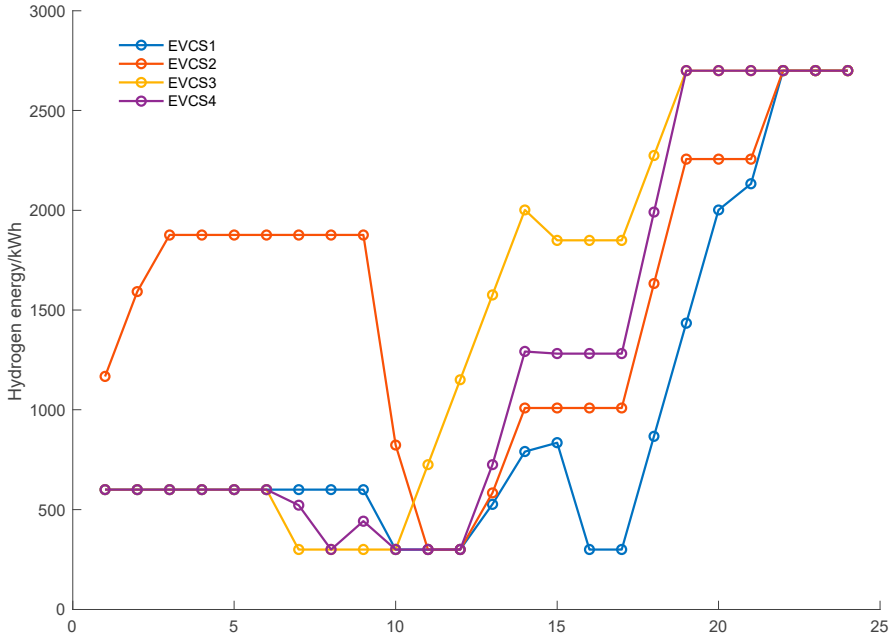

Figure 12. Four SHS-EVCSs' hydrogen usage.

Figure 13 shows an optimization of charging over a 24 h period and how electricity is used throughout the day at four different SHS-EVCSs. The differentiated color within the stacked bar graph distinctly demarcates the electricity usage attributable to each SHS-EVCS, with the proportional segment heights within each hourly bar representing the specific electricity consumption metrics. Upon comparative analysis with Figure 6, which presumably delineates the EV charging quantities at corresponding intervals, a correlative trend emerges. The electricity usage profile depicted in the current figure exhibits parallel fluctuations to the charging activities recorded in Figure 6, suggesting a direct relationship between the electricity consumed by the SHS-EVCSs and the operational charging volume.

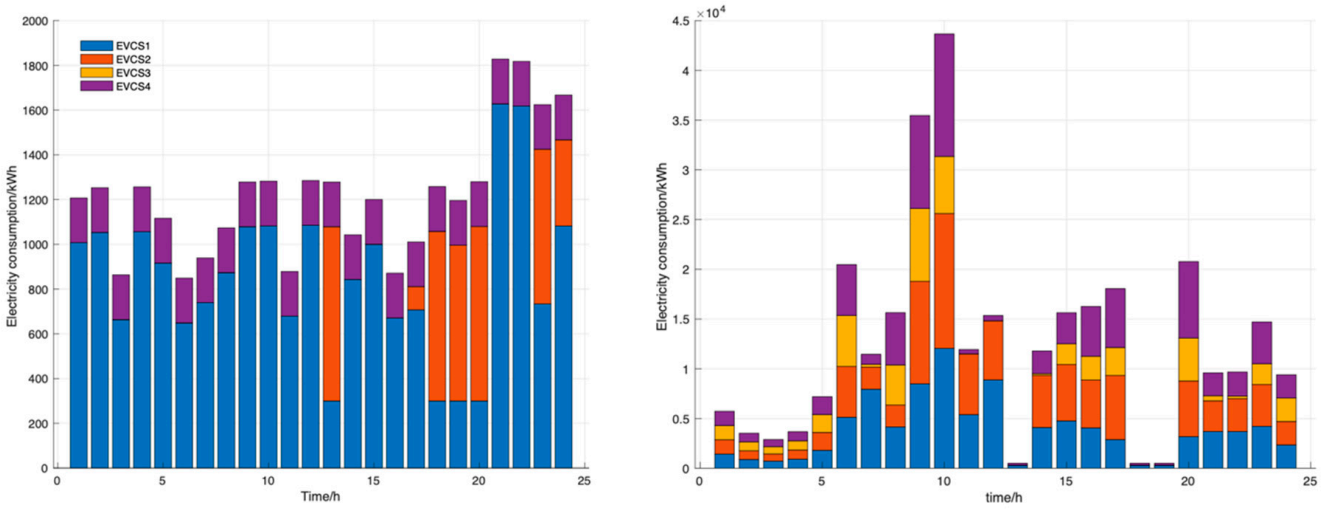

a b.

Figure 13. Four SHS-EVCSs' EV charging optimization over 24 h: (**a**) weekends; (**b**) weekdays.

Each figure in Figure 14 indicates the buyer and seller (for example, "EVCS1 purchases from EVCS2" suggests that source EVCS1 is buying from source EVCS2) with time represented in 24 h. The data points are connected by lines to indicate the change in purchasing activity over time:

(a) EVCS1 purchases from EVCS2: This figure shows the variation in purchases made by source EVCS1 from source EVCS2 over time. There are several distinct peaks in purchasing activity, especially around 3 a.m. and 6 a.m.
(b) EVCS1 purchases from EVCS3: In this figure, purchasing activity by source EVCS1 from source EVCS3 also shows several peaks, particularly at 2 a.m., 4 a.m., 6 a.m., and 9 a.m.
(c) EVCS1 purchases from EVCS4: This figure shows peaks in purchases by source EVCS1 from source EVCS4 at 1 a.m., 5 a.m., 8 a.m., and 12 p.m.
(d) EVCS2 purchases from EVCS1: EVCS2's purchases from source EVCS1 show peaks from 2 a.m. to 12 p.m.
(e) EVCS2 purchases from EVCS3: This figure displays several peaks in purchases by source EVCS2 from source EVCS3, especially at 6 a.m.
(f) EVCS2 purchases from EVCS4: In this figure, source EVCS2's purchases from source EVCS4 peak at 5 a.m.
(g) EVCS3 purchases from EVCS1: Purchases by source EVCS3 from source EVCS1 are higher between 2 a.m. and 12 p.m.
(h) EVCS3 purchases from EVCS2: In this figure, source EVCS3's purchases from source EVCS2 show notable peaks at 2 a.m. and 5 a.m.
(i) EVCS3 purchases from EVCS4: This figure indicates that source EVCS3's purchases from source EVCS4 peak before 12 p.m.
(j) EVCS4 purchases from EVCS1: Source EVCS4's purchases from source EVCS1 show peaks at 12 p.m.
(k) EVCS4 purchases from EVCS2: In this figure, source EVCS4's purchases from source EVCS2 peak at 10 a.m. and 12 a.m.
(l) EVCS4 purchases from EVCS3: Source EVCS4's purchases from source EVCS3 have peaks at 4 a.m., 10 a.m. and 11 a.m.

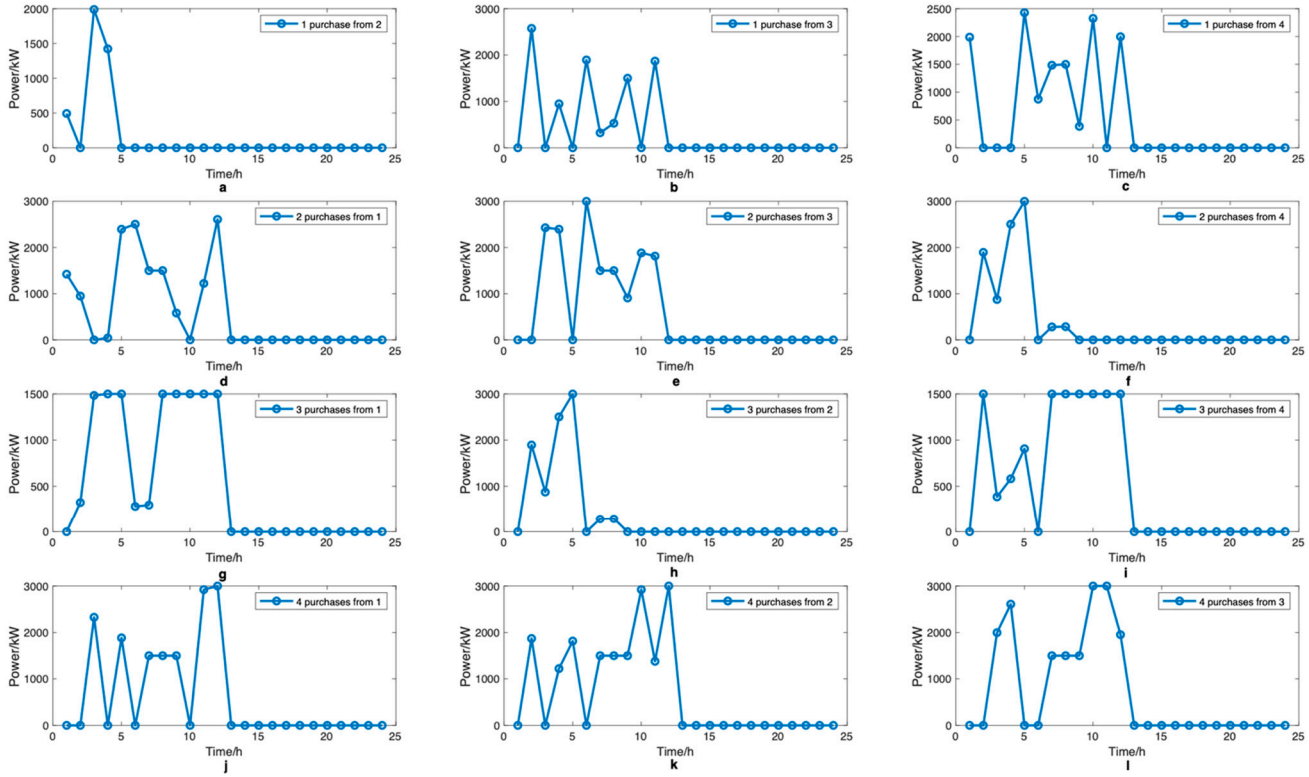

Figure 14. P2P trading strategy between 4 SHS-EVCSs. (**a**) EVCS1 purchases from EVCS2, (**b**) EVCS1 purchases from EVCS3, (**c**) EVCS1 purchases from EVCS4, (**d**) EVCS2 purchases from EVCS1, (**e**) EVCS2 purchases from EVCS3, (**f**) EVCS2 purchases from EVCS4, (**g**) EVCS3 purchases from EVCS1, (**h**) EVCS3 purchases from EVCS2, (**i**) EVCS3 purchases from EVCS4, (**j**) EVCS4 purchases from EVCS1, (**k**) EVCS4 purchases from EVCS2, and (**l**) EVCS4 purchases from EVCS3.

These figures represent the fluctuation of transaction volumes between different suppliers or products over time. Peaks can indicate high demand or bulk transactions at specific points in time. Analyzing these figures could provide insights into the patterns and trends of trade activity between different sources, which may be valuable for optimizing inventory management, forecasting future demands, or adjusting supply chain strategies.

Figure 15 shows the cost comparison between internal electricity purchasing and grid procurement for SHS-EVCSs. The figure demonstrates that the price of internal energy trading daily is more economical than solely relying on electricity purchased from the grid. This comparison highlights the financial advantages of internal trading within SHS-EVCSs, underlining the potential for significant cost savings by optimizing internal electricity transactions over external grid procurement. It provides a clear visual representation of the cost-effectiveness of leveraging internal energy resources, encouraging the adoption of such strategies to enhance economic efficiency in SHS-EVCS operations.

The economic analysis presented here is critical not only for understanding the economic feasibility of SHS-EVCS configurations but also for decision-making related to the scaling and expansion of such systems. The notable disparity between the total daily costs and revenues highlights the potential for considerable profit generation, which can be instrumental in driving investment decisions and fostering the broader adoption of renewable energy technologies within the electric vehicle charging infrastructure.

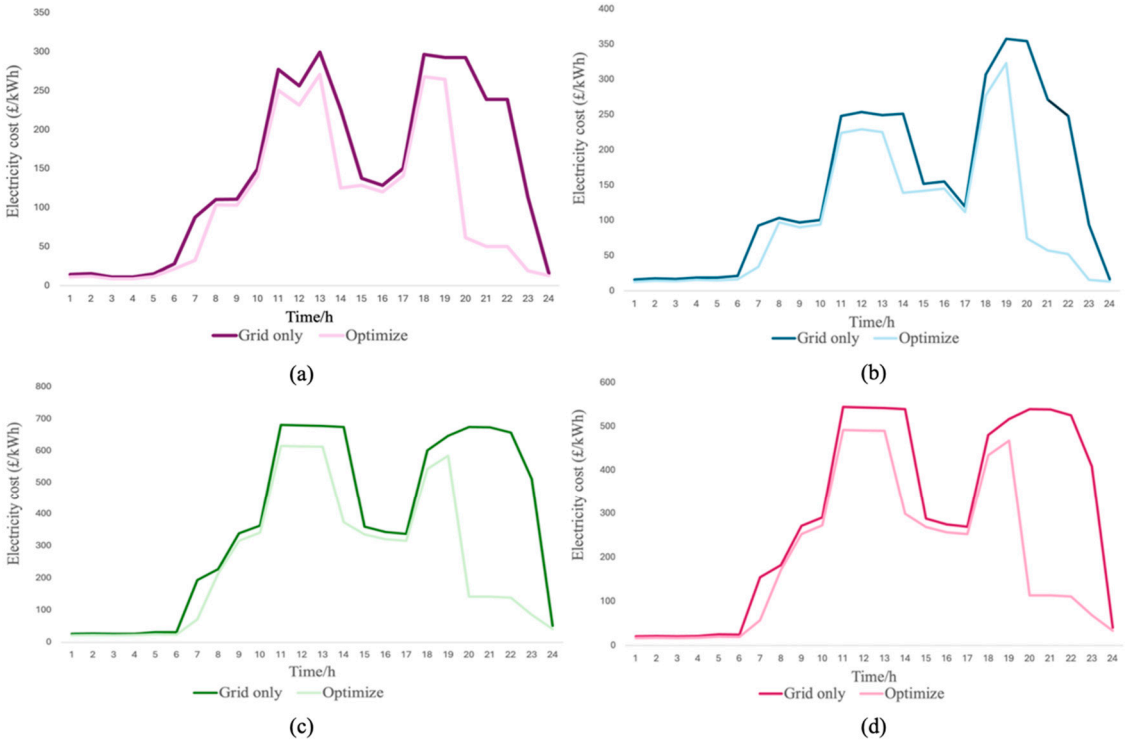

Figure 15. Comparison of internal electricity purchasing versus grid procurement for SHS-EVCSs. (**a**) EVCS1, (**b**) EVCS2, (**c**) EVCS3, and (**d**) EVCS4.

6. Conclusions

This paper introduces a P2P transactive energy trading strategy tailored for multi-SHS-EVCSs, with a particular focus on addressing the challenges posed by the inherent intermittency and volatility of RE generation. This innovative strategy is designed to mitigate the uncertainties arising from inaccurate renewable energy forecasts, which can significantly impact the operational efficiency and economic viability of SHS-EVCSs. A notable advancement presented in this paper is the P2P based cooperative game-theoretical approaches. This agreement acts as a mechanism to resolve conflicts of interest, ensuring that all participating SHS-EVCSs collaborate towards mutual benefit. Such collaboration is crucial for stabilizing the system and preventing any single SHS-EVCS from altering its game strategy—such as electricity pricing strategies—in a manner that could destabilize the system. Overall, the proposed energy trading strategy not only enhances the operational efficiency of SHS-EVCSs but also fosters a cooperative environment that ensures the long-term sustainability and economic efficiency of renewable energy utilization in electric vehicle charging infrastructures.

This study has several limitations that warrant further exploration. Primarily, it does not incorporate demand-side management strategies, notably demand response, into its framework. Moreover, the research overlooks critical distinctions between cooperative and non-cooperative game-theoretical approaches, which could influence the outcomes. Additionally, aspects of social welfare, such as EV driver's welfare, have not been adequately considered. Consequently, future research will need to address these gaps to refine the robustness and applicability of the findings in a broader context.

Author Contributions: Conceptualization, L.D. and C.S.L.; methodology, L.D., Y.Y. and C.S.L.; software, L.D.; validation, L.D.; formal analysis, L.D. and Y.Y.; investigation, L.D.; resources, L.D.; data curation, L.D.; writing—original draft preparation, L.D.; writing—review and editing, L.D., Y.Y., C.S.L. and G.T.; visualization, L.D.; supervision, C.S.L. and G.T.; project administration, C.S.L. and G.T. All authors have read and agreed to the published version of the manuscript.

Funding: This research received no external funding.

Data Availability Statement: Data are contained within the article.

Conflicts of Interest: The authors declare no conflicts of interest.

Nomenclature

$E_{AE,t}$	Hydrogen produced by the electrolyzer, kWh
$P_{AE.t}$	Electrical power consumed by the electrolyzer, kW
ν	Hydrogen conversion efficiency, 75%
a	Conversion coefficient for electric energy to the equivalent energy in hydrogen, 39.65 kWh/kg
P_{FC}	Output power of the fuel cell, kW
E_{FC}	Hydrogen consumed by the fuel cell, kWh
η_{FC}s	Energy conversion coefficient for fuel cell, 70%
$E_{hs}(t)$	Total quantity of hydrogen stored in the hydrogen tank at time t, kWh
$E_{hs}(t-1)$	Total quantity of hydrogen stored in the hydrogen tank at time $t-1$, kWh
δ_{hs}	Energy storage decay rate of the hydrogen tank, 5%
$E_{hs}^{in}(t)$	Input quantity of hydrogen into the hydrogen tank, kWh
$E_{hs}^{out}(t)$	Output quantity of hydrogen from the hydrogen tank, kWh
η_{hs}^{in}	Input efficiency of the hydrogen tank, 98%
η_{hs}^{out}	Output efficiency of the hydrogen tank, 98%
P_{STC}	Rated output power of the PV components under standard test conditions
G_{AC}	Real-time solar irradiance intensity
T_c	Real-time temperature of the photovoltaic component surface
G_{STC}	Illumination under standard test conditions, 1000 W/m^2
T_r	25 °C
T_a	Ambient temperature
T_N	*PV* cell operating temperature
$E_{BSS}(c)$	Energy of the battery at the c-th time, kWh
$E_{gen}(c)$	Energy generated by the generator at the c-th time
$E_{load}(c)$	Energy of the load at the c-th time
e_{inv}	Efficiency of the inverter, 95%
η_b^{ch}	Charging efficiency of the battery, 80%
η_b^{dch}	Discharging efficiency of the battery, 80%
$C_{n,t}^{E_H}$	Hydrogen cost, GBP
$C_{n,t}^{FC}$	Fuel cell generator cost, GBP
$C_{n,t}^{grid}$	Grid cost, GBP
$C_{n,t}^{Pv}$	Solar cost, GBP
$C_{n,t}^{p2p}$	P2P trading cost, GBP
C_t^{Bes}	Battery energy storage cost, GBP
$C_{n,t}^{sell}$	Sale revenue, GBP
$\rho_{n,t}^{B}$	P2P trading price by SHS-EVCS n from grid at time t, GBP/kWh
$E_{n,t}^{B}$	P2P trading power by SHS-EVCS n from grid at time t, kWh
$\rho_{n,t}^{g}$	P2P trading price by grid from SHS-EVCS at time t, GBP/kWh
$E_{n,t}^{g}$	P2P trading power by grid from SHS-EVCS at time t, kWh
$\rho_{n,t}^{inter}$	The price of number n SHS-EVCS selling electricity to other SHS-EVCS using internal load, GBP/kWh
$E_{n,t}^{g}$	SHS-EVCSs buying electricity from grid, GBP/kWh
$E_{n,t}^{g*}$	SHS-EVCSs selling electricity to grid, GBP/kWh
$E_{in,t}^{cs}$	SHS-EVCS i follow the SHS-EVCS n pricing rule to buying power at time t, kWh
$\rho_{n,t}^{cs}$	Pricing rule, GBP/kWh

$E_{n,t}^{load}$	Internal load demand of SHS-EVCS, kWh
$E_{n,t}^{i}$	P2P trading power between SHS-EVCS n and I, kWh
$E_{i,t}^{n}$	P2P trading power between SHS-EVCS i and n, kWh
$u_{hs}(t)$	State variable of the electrolyzer
$E_{hs,min}^{o}$	Lower output limit of the electrolyzer, kWh
$E_{hs,max}^{o}$	Upper output limit of the electrolyzer, kWh
$E_{hs,min}^{in}$, $E_{hs,max}^{in}$	Lower and upper input limit of the electrolyzer, kWh
$E_{hs,min}^{out}$, $E_{hs,max}^{out}$	Lower and upper output limit of the electrolyzer, kWh
u_{hs}^{in}	Hydrogen tank storage state variable
u_{hs}^{out}	Hydrogen tank release state variable.
$P_{FC,max}^{out}$	Maximum power output for fuel cell generator, kW
$P_{pv,\,min}$, $P_{pv,\,max}$	Minimum and maximum PV power output, kW
E_{rate_BSS}	Self-discharge rate of the battery
DOD	Depth of discharge, 0.9
Abbreviations	
EV	Electric vehicle
CSs	Charging stations
SHS-EVCSs	Solar-Hydrogen-Battery Storage Electric Vehicle Charging Stations
P2P	Peer to peer
PV	Photovoltaic
RE	Renewable energy
SoC	State of charge
DER	Distributed energy resource
DRP	Demand response program
MILP	Mixed integer linear programming.
DOD	Depth of discharge
P2G	Power to gas
G2P	Gas to power

References

1. Sun, B. A multi-objective optimization model for fast electric vehicle charging stations with wind, PV power and energy storage. *J. Clean. Prod.* **2021**, *288*, 125564. [CrossRef]
2. Merhy, G.; Nait-Sidi-Moh, A.; Moubayed, N. A multi-objective optimization of electric vehicles energy flows: The charging process. *Ann. Oper. Res.* **2021**, *296*, 315–333. [CrossRef]
3. Shahalami, S.; Ahmadnia, S.; Armanfard, S. Locating electric vehicle solar charging and discharging stations using multi-objective genetic algorithm and fuzzy decision making. *Appl. Sol. Energy* **2022**, *58*, 177–186. [CrossRef]
4. Bouguerra, S.; Bhar Layeb, S. Determining optimal deployment of electric vehicles charging stations: Case of Tunis City, Tunisia. *Case Stud. Transp. Policy* **2019**, *7*, 628–642. [CrossRef]
5. Awasthi, A.; Venkitusamy, K.; Padmanaban, S.; Selvamuthukumaran, R.; Blaabjerg, F.; Singh, A. Optimal planning of electric vehicle charging station at the distribution system using hybrid optimization algorithm. *Energy* **2017**, *133*, 70–78. [CrossRef]
6. Mera, L. Application of the Montecarlo simulation for the implementation analysis of fast charging stations for electric vehicles in the Galapagos Province. *Rev. Energ. CENACE* **2021**, *17*, 143–152.
7. Liu, Z.; Song, J.; Kubal, J.; Susarla, N.; Knehr, K.W.; Islam, E.; Nelson, P.; Ahmed, S. Comparing total cost of ownership of battery electric vehicles and internal combustion engine vehicles. *Energy Policy* **2021**, *158*, 112564. [CrossRef]
8. Muratori, M.; Alexander, M.; Arent, D.; Bazilian, M.; Cazzola, P.; Dede, E.M.; Farrell, J.; Gearhart, C.; Greene, D.; Jenn, A.; et al. The rise of electric vehicles—2020 status and future expectations. *Prog. Energy* **2021**, *3*, 022002. [CrossRef]
9. Johnson, L.; Marke, A. The Revival of Electric Vehicles: Historical Perspectives and Modern Advances. *J. Mod. Transp.* **2023**, *31*, 120–135.
10. Zhou, Y.; Lund, P.D. Peer-to-peer energy sharing and trading of renewable energy in smart communities–trading pricing models decision-making and agent-based collaboration. *Renew. Energy* **2023**, *207*, 177–193. [CrossRef]
11. Luo, X.; Shi, W.; Jiang, Y.; Liu, Y.; Xia, J. Distributed peer-to-peer energy trading based on game theory in a community microgrid considering ownership complexity of distributed energy resources. *J. Clean. Prod.* **2022**, *351*, 131573. [CrossRef]
12. Kong KG, H.; Lim, J.Y.; Leong, W.D.; Ng WP, Q.; Teng, S.Y.; Sunarso, J.; How, B.S. Fuzzy optimization for peer-to-peer (P2P) multi-period renewable energy trading planning. *J. Clean. Prod.* **2022**, *368*, 133122. [CrossRef]
13. Yan, X.; Song, M.; Cao, J.; Gao, C.; Jing, X.; Xia, S.; Ban, M. Peer-to-Peer transactive energy trading of multiple microgrids considering renewable energy uncertainty. *Int. J. Electr. Power Energy Syst.* **2023**, *152*, 109235. [CrossRef]

14. Chen, B.; Che, Y.; Zhou, Y.; Zhao, S. Day-ahead optimal peer-to-peer energy trading strategy for multi-microgrids based on Nash bargaining game with data-driven chance constraints. *Sustain. Energy Grids Netw.* **2023**, *36*, 101192. [CrossRef]
15. Gunarathna, C.L.; Yang, R.J.; Jayasuriya, S.; Wang, K. Reviewing global peer-to-peer distributed renewable energy trading projects. *Energy Res. Soc. Sci.* **2022**, *89*, 102655. [CrossRef]
16. Liu, W.; Xu, H.; Wang, X.; Zhang, S.; Hu, T. Optimal dispatch strategy of virtual power plants using potential game theory. *Energy Rep.* **2022**, *8*, 1069–1079. [CrossRef]
17. Choobineh, M.; Arabnya, A.; Khodaei, A.; Zheng, H. Game-theoretic peer-to-peer solar energy trading on blockchain-based transaction infrastructure. *Adv. Electr. Eng. Electron. Energy* **2023**, *5*, 100192. [CrossRef]
18. Goudarzi, A.; Li, Y.; Fahad, S.; Xiang, J. A game theory-based interactive demand response for handling dynamic prices in security-constrained electricity markets. *Sustain. Cities Soc.* **2021**, *72*, 103073. [CrossRef]
19. Mousavizadeh, S.; Haghifam, M.-R.; Shariatkhah, M.-H. A linear two-stage method for resiliency analysis in distribution systems considering renewable energy and demand response resources. *Appl. Energy* **2018**, *211*, 443–460. [CrossRef]
20. Chawal, U.; Rosenberger, J.; Chen VC, P.; Lee, W.J.; Wijemanne, M.; Punugu, R.K.; Kulvanitchaiyanunt, A. A design and analysis of computer experiments based mixed integer linear programming approach for optimizing a system of electric vehicle charging stations. *Expert Syst. Appl.* **2024**, *245*, 123064. [CrossRef]
21. Adouani, Y.; Masmoudi, M.; Jarray, F.; Jarboui, B. Iterative integer linear programming-based heuristic for solving the multiple-choice knapsack problem with setups. *Expert Syst. Appl.* **2024**, *242*, 122835. [CrossRef]
22. Selvam, S.K.; Rajendran, C.; Sankaralingam, G. A linear programming-based bi-objective optimization for forecasting short univariate time series. *Decis. Anal. J.* **2024**, *10*, 100400. [CrossRef]
23. Teng, F.; Zhang, Q.; Xiao, G.; Ban, Z.; Liang, Y.; Guan, Y. Energy Management for a Port Integrated Energy System Based on Distributed Dual Decomposition Mixed Integer Linear Programming. *J. Mar. Sci. Eng.* **2023**, *11*, 1137. [CrossRef]
24. Lee, W.; Han, D.; Won, D. Grid-Oriented Coordination Strategy of Prosumers Using Game-theoretic Peer-to-Peer Trading Framework in Energy Community. *Appl. Energy* **2022**, *326*, 119980. [CrossRef]
25. Yu, X.; Pan, D.; Zhou, Y. A Stackelberg game-based peer-to-peer energy trading market with energy management and pricing mechanism: A case study in Guangzhou. *Sol. Energy* **2024**, *270*, 112388. [CrossRef]
26. Li, Z.; Wu, L.; Xu, Y.; Wang, L.; Yang, N. Distributed tri-layer risk-averse stochastic game approach for energy trading among multi-energy microgrids. *Appl. Energy* **2023**, *331*, 120282. [CrossRef]
27. Paudel, A.; Chaudhari, K.; Long, C.; Gooi, H. Peer-to-Peer Energy Trading in a Prosumer-Based Community Microgrid: A Game-Theoretic Model. *IEEE Trans. Ind. Electron.* **2019**, *66*, 6087–6097. [CrossRef]
28. Malik, S.; Duffy, M.; Thakur, S.; Hayes, B.; Breslin, J. A priority-based approach for peer-to-peer energy trading using cooperative game theory in local energy community. *Int. J. Electr. Power Energy Syst.* **2022**, *137*, 107865. [CrossRef]
29. Li, Z.; Lei, X.; Shang, Y.; Jia, Y.; Jian, L. A Vehicle-to-Vehicle Energy Trading System for Electric Vehicle Networks: A Non-Cooperative Game Approach. *J. Clean. Prod.* **2015**, *414*, 567–589.
30. Liu, Z.; Wu, Q.; Huang, S.; Wang, L.; Shahidehpour, M.; Xue, Y. Optimal Day-Ahead Charging Scheduling of Electric Vehicles Through an Aggregative Game Model. *IEEE Trans. Smart Grid* **2018**, *9*, 5173–5184. [CrossRef]
31. Spiliopoulos, N.; Sarantakos, I.; Nikkhah, S.; Gkizas, G.; Giaouris, D.; Taylor, P.; Rajarathnam, U.; Wade, N. Peer-to-peer energy trading for improving economic and resilient operation of microgrids. *Renew. Energy* **2022**, *199*, 517–535. [CrossRef]
32. Liu, W.; Gu, W.; Wang, J.; Yu, W.; Xi, X. Game Theoretic Non-Cooperative Distributed Coordination Control for Multi-Microgrids. *IEEE Trans. Smart Grid* **2018**, *9*, 6986–6997. [CrossRef]
33. Jing, R.; Xie, M.; Wang, F.; Chen, L. Fair P2P energy trading between residential and commercial multi-energy systems enabling integrated demand-side management. *Appl. Energy* **2020**, *262*, 114551. [CrossRef]
34. Bhatti, B.; Broadwater, R. Energy trading in the distribution system using a non-model based game theoretic approach. *Appl Energy* **2019**, *253*, 113532. [CrossRef]
35. Duan, L.; Guo, Z.; Taylor, G.; Lai, C.S. Multi-Objective Optimization for Solar-Hydrogen-Battery-Integrated Electric Vehicle Charging Stations with Energy Exchange. *Electronics* **2023**, *12*, 4149. [CrossRef]
36. Sapountzi, F.; Gracia, J.; Weststrate, C.; Kee, J.; Fredriksson, H.; Niemantsverdriet, J. Electrocatalysts for the generation of hydrogen, oxygen and synthesis gas. *Prog. Energy Combust. Sci.* **2017**, *58*, 1e35. [CrossRef]
37. Li, N.; Zhao, X.; Shi, X.; Pei, Z.; Mu, H.; Taghizadeh-Hesary, F. Integrated energy systems with CCHP and hydrogen supply: A new outlet for curtailed wind power. *Appl. Energy* **2021**, *303*, 117619. [CrossRef]
38. Ishaq, H.; Dincer, I.; Crawford, C. A review on hydrogen production and utilization: Challenges and opportunities. *Int. J. Hydrogen Energy* **2022**, *47*, 26238e64. [CrossRef]
39. Taleb, B.; Jahjah, R.; Cornu, D.; Bechelany, M.; Al Ajami, M.; Kataya, G.; Hijazi, A.; El-Dakdouki, M.H. Exploring Hydrogen Sources in Catalytic Transfer Hydrogenation: A Review of Unsaturated Compound Reduction. *Molecules* **2023**, *28*, 7541. [CrossRef]
40. Abdelshafy, A.M.; Hassan, H.; Jurasz, J. Optimal design of a grid-connected desalination plant powered by renewable energy resources using a hybrid PSO–GWO approach. *Energy Convers. Manag.* **2018**, *173*, 331–347. [CrossRef]
41. Churkin, A.; Bialek, J.; Pozo, D.; Sauma, E.; Korgin, N. Review of Cooperative Game Theory applications in power system expansion planning. *Renew. Sustain. Energy Rev.* **2021**, *145*, 111056. [CrossRef]
42. China Solar Panel Costs Drop 42% from Year Ago—Report. Reuters. Available online: https://www.reuters.com/world/china/china-solar-panel-costs-drop-42-year-ago-report-2023-12-14/ (accessed on 14 December 2023).

43. Battery Prices Collapsing, Grid-Tied Energy Storage Expanding. PV Magazine. Available online: https://www.pv-magazine.com/2024/03/07/battery-prices-collapsing-grid-tied-energy-storage-expanding/#:~:text=Since%20last%20summer,%20lithium%20battery,/kWh%20to%20$130/kWh (accessed on 7 March 2024).
44. Yin, I. China Targets to Cut Battery Storage Costs by 30% by 2025. S&P Global Commodity Insights. Available online: https://www.spglobal.com/commodityinsights/en/market-insights/latest-news/energy-transition/032222-china-targets-to-cut-battery-storage-costs-by-30-by-2025#:~:text=China's%20electrochemical%20energy%20storage%20cost,the%20Chinese%20Academy%20of%20Sciences (accessed on 22 March 2022).